

AD A 050681

NWC TP 5997

12  
K

# Variations in Optical Reflectivity of Sputter Deposited Metal and Semimetal Films

by  
H. F. Blazek  
G. H. Turner  
C. W. Cutsinger  
*Engineering Department*

DECEMBER 1977

Approved for public release; distribution unlimited.

DDDC  
RECEIVED  
MAR 2 1978  
F

AD NO. 1  
DGC FILE COPY

## Naval Weapons Center

CHINA LAKE, CALIFORNIA 93555



# Naval Weapons Center

AN ACTIVITY OF THE NAVAL MATERIAL COMMAND

## FOREWORD

The research described in this effort was performed and funded by the Engineering Department during fiscal year 1975. It is part of a continuing effort to develop techniques and applications of thin-film coatings for infrared weapons systems and/or infrared missile detector systems.

This report has been reviewed for technical accuracy by G. H. Turner.

Approved by  
G. W. LEONARD, *Head*  
*Engineering Department*  
28 December 1977

Under authority of  
W. L. HARRIS, JR.  
RAdm., U.S. Navy  
*Commander*

Released for publication by  
R. M. Hillyer  
*Technical Director*

NWC Technical Publication 5997

Published by ..... Technical Information Department  
Collation ..... Cover, 11 leaves  
First printing ..... 235 unnumbered copies

- 1 Lockheed Missiles and Space Company, Sunnyvale, CA (L. R. Lunsford)
- 1 McDonnell Douglas Astronautics Company, Huntington Beach, CA  
(Department A3-8. -BBFO, P. L. Klevatt)
- 1 McDonnell Douglas Corporation, St. Louis, MO (Department 220,  
Dr. D. P. Ames)
- 2 Martin Company, Denver, CO  
Steward Chapin (1)  
Scott Giles (1)
- 2 Mathematical Sciences Northwest, Bellevue, WA  
Dr. Abraham Hertzberg (1)  
Peter H. Rose (1)
- 1 Mitre Corporation, Bedford, MA (A. C. Cron)
- 1 Northrop Corporation, Norair Division, Hawthorne, CA  
(Laser Systems Department, Dr. Gerard Hasserjian)
- 2 Oak Ridge National Laboratory, Oak Ridge, TN  
Dr. E. T. Arakawa (1)  
Research Materials Information Center (1)
- 1 Physics International, San Leandro, CA (Director, Applied  
Science Department, E. T. Moore)
- 2 R&D Associates, Marina del Rey, CA  
Dr. R. Hundley (1)  
Dr. R. E. LeLevier (1)
- 1 Radio Corporation of America, Moorestown, NJ (Systems Projects,  
J. J. Mayman)
- 1 Raytheon Company, Waltham, MA (Research Division, Dr. Frank A. Horrigan)
- 3 Riverside Research Institute, New York, NY  
Dr. John Bose (1)  
Dr. L. H. O'Neill (1)  
HPEGL Library, Helen Gressman (1)
- 2 Stanford Research Institute, Menlo Park, CA  
Dr. H. E. Lindberg (1)  
J. E. Malick (1)
- 1 TRW, Inc., Redondo Beach, CA (Norman Campbell)
- 2 The Boeing Company, Seattle, WA (Dr. E. K. Bjornerud)
- 1 The Rand Corporation, Santa Monica, CA (Dr. Claude R. Culp/S. A. Carter)
- 1 Thiokol Chemical Corporation, Wasatch Division, Brigham City, UT  
(J. M. Mason)
- 4 United Aircraft Corporation, East Hartford, CT  
Albert Angelbeck (1)  
G. H. McLafferty (3)
- 3 United Aircraft Corporation, West Palm Beach, FL  
Dr. R. A. Schmidtke (1)  
Ed Pinsley (1)
- 4 University of Arizona, Optical Science Center, Tucson, AZ  
Dr. B. O. Seraphim (1)  
Dr. Francis Turner (1)

Dr. William L. Wolfe (1)

C. L. Blenman (1)

3 University of California, Lawrence Radiation Laboratory, Livermore, CA

Dr. Joe Fleck (1)

Dr. R. E. Kidder (1)

Dr. E. Teller (1)

1 VARIAN Associates, San Carlos, CA (EIMAC Division, Jack Quinn)

1 Vought, Inc., Systems Division, Dallas, TX (F. G. Simpson)

3 Westinghouse Defense and Space Center, Baltimore, MD (R. A. Lee)

1 Westinghouse Electric Corporation, Research and Development Laboratories,  
Pittsburgh, PA (E. P. Reidel)

UNCLASSIFIED

SECURITY CLASSIFICATION OF THIS PAGE (When Data Entered)

REPORT DOCUMENTATION PAGE		READ INSTRUCTIONS BEFORE COMPLETING FORM
1. REPORT NUMBER <b>14</b> NWC-TP-5997 ✓	2. GOVT ACCESSION NO.	3. RECIPIENT'S CATALOG NUMBER
4. TITLE (and Subtitle) <b>6</b> VARIATIONS IN OPTICAL REFLECTIVITY OF SPUTTER DEPOSITED METAL AND SEMIMETAL FILMS.	5. TYPE OF REPORT & PERIOD COVERED <b>9</b> Summary report, for <b>12</b> 1975	
7. AUTHOR(s) <b>10</b> H. F. Blazek, G. H. Turner, and C. W. Cutsinger	6. PERFORMING ORG. REPORT NUMBER	
9. PERFORMING ORGANIZATION NAME AND ADDRESS Naval Weapons Center ✓ China Lake, CA 93555	8. CONTRACT OR GRANT NUMBER(s)	
11. CONTROLLING OFFICE NAME AND ADDRESS Naval Weapons Center China Lake, CA 93555	10. PROGRAM ELEMENT, PROJECT, TASK AREA & WORK UNIT NUMBERS	
14. MONITORING AGENCY NAME & ADDRESS (if different from Controlling Office)	12. REPORT DATE <b>11</b> Dec 1977	13. NUMBER OF PAGES 20 <b>12</b> 20p.
	15. SECURITY CLASS. (of this report) UNCLASSIFIED	
16. DISTRIBUTION STATEMENT (of this Report) Approved for public release; distribution unlimited.	15a. DECLASSIFICATION/DOWNGRADING SCHEDULE	
17. DISTRIBUTION STATEMENT (of the abstract entered in Block 20, if different from Report)	DDC APPROVED MAR 2 1978 RECEIVED F	
18. SUPPLEMENTARY NOTES		
19. KEY WORDS (Continue on reverse side if necessary and identify by block number) Metal Films, Sputter Deposited Optical Reflectivity, Films Semimetal Films, Sputter Deposited		
20. ABSTRACT (Continue on reverse side if necessary and identify by block number) See back of form.		

UNCLASSIFIED

SECURITY CLASSIFICATION OF THIS PAGE(When Data Entered)

(U) *Variations in Optical Reflectivity of Sputter Deposited Metal and Semimetal Films* by H. F. Blazek, G. H. Turner, and C. W. Cutsinger, China Lake, Calif., Naval Weapons Center, December 1977. 20 pp. (NWC TP 5997, publication UNCLASSIFIED.)

(U) The surface structure of vacuum sputter deposited metal and semimetal films can be varied by changing the substrate bias potential and the total time of deposition. The corresponding change in the optical reflectivity can be related to enhanced scattering and absorption effects. Reflectivity measurements over the infrared range from 1 to 7 microns are presented and discussed for titanium, antimony, bismuth, and copper films. Results for the metal films, copper and titanium, are in agreement with those obtained by Bennett for aluminum films. The results for antimony and bismuth indicate the influence of enhanced absorption.



ACCESS FOR	Section <input checked="" type="checkbox"/>
NTIS	Section <input type="checkbox"/>
DDC	Section <input type="checkbox"/>
U.S.C.	
DISTRIBUTION/AVAILABILITY STATEMENTS	
A	

UNCLASSIFIED

## INTRODUCTION

The surface structure of vacuum sputter deposited metal and semimetal films can be varied by changing either the substrate bias or the total time of the deposition. Reflectivity data for titanium, bismuth, antimony, and copper films are examined and features of these curves related to surface scattering and possible enhanced absorption effects.

## DEPOSITION TECHNIQUE

Films of titanium, bismuth, antimony, and copper were bias sputtered in a Varian Model 980-2404 chamber mounted on a standard Inovac pumping station. Initially films were deposited using a combination of various bias settings and deposition times. The objective was to determine which particular set of parameters produced films that scattered or absorbed very strongly in the visible spectrum. Once this was determined, a set of samples was prepared for reflectivity measurements over the range of 1 to 7 microns. The substrates were polished quartz. The smooth films were prepared by sputtering a continuous film about 500 to 800 angstroms thick. Argon was used as the sputtering gas. Figure 1 is a schematic of the arrangement used to obtain the films. Scanning electron micrographs were taken of the samples. Figures 2 through 6 illustrate the structures obtained for bismuth films.

The bismuth film shown in Figures 2 and 3 was sputter deposited on polished quartz at zero potential bias and with an argon pressure of  $3 \times 10^{-2}$  torr. The average size of the smaller protuberances is 1.2 microns and the larger ones average 15 microns in width. The appearance of small particles surrounded by rings of larger particles suggests that a diffusion process may be taking place in which the larger particles grow at the expense of the smaller particles. The film shown in Figures 4 and 5 verifies this growth characteristic. The larger protuberances average 127 microns in diameter. Preparation of this film differed from that shown previously only in length of deposition time. The deposition time in this case was doubled.

The influence of a crystalline substrate on this growth characteristic is illustrated in Figure 6. Here the deposition was similar to that for the bismuth film shown in Figure 2 except that the substrate is single-crystal sapphire. The effect of the substrate structure is to promote crystalline growth of the bismuth within the individual protuberances. The average width of these projections is 12 microns, very nearly the same as the average width of the larger particles grown on the quartz substrate.

## REFLECTIVITY DATA

Reflectivity data for aluminum films deposited onto intentionally roughened substrates obtained by Bennett is shown in Figure 7.<sup>1</sup> This data indicates that for rougher films the point at which reflectivity becomes apparent shifts to longer wavelengths and a reduction in reflectivity occurs. These characteristics are attributed to scattering by the surface protuberances. A shift to longer wavelengths and reduction in reflectivity is also seen in the data obtained (by the authors) for bias sputtered bismuth and copper shown in Figures 8 and 9 and Tables 1 and 2. Reflectivity of titanium and antimony also display these characteristics (Figures 10 and 11 and Tables 3 and 4). The data indicates that a rather abrupt change in the relative reflectance occurs between 3.0 and 4.0 microns for the titanium and between 3.5 and 4.5 for antimony (Figures 12 and 13). Note that for bismuth the relative reflectance curve is a smooth function (Figure 14).

TABLE 1. Relative Reflectance  
of Smooth and Rough  
Sputtered Bismuth.

$\lambda$	$R_{\text{smooth}}$	$R_{\text{rough}}$
1.0	0.22482	0.00000
1.5	.39548	.01633
2.0	.47071	.01740
2.5	.49830	.04192
3.0	.51854	.07244
3.5	.53485	.12104
4.0	.54538	.17219
4.5	.55352	.21533
4.7	.55688	.22590
4.75	.55695	.22972
4.8	.55712	.23319
5.0	.56028	.24480
5.5	.56623	.27171
6.0	.57207	.29517
6.5	.57314	.31396
7.0	.57429	.32568

TABLE 2. Relative  
Reflectance of  
Rough Copper.

$\lambda$	$R_{\text{rough}}$
1.0	0.00000
1.5	.00000
2.0	.00000
2.5	.02514
3.0	.06108
3.5	.17740
4.0	.29728
4.5	.37421
4.7	.39604
4.75	.40516
4.8	.40854
5.0	.42441
5.5	.45789
6.0	.46618
6.5	.47504
7.0	.48564

## RESONANT DIPOLE ABSORPTION

This additional change in reflectivity of titanium and antimony films may possibly be associated with enhanced absorption due to a resonant dipole mechanism (surface plasmon effect). The resonant dipole model as described by Decker considers polarizable oblate spheroids elevated above a reflecting plane.<sup>2</sup> These spheroids are an approximation to the actual protuberances observed on a real film.

<sup>1</sup> H. E. Bennett, "Specular Reflectance of Aluminized Ground Glass and the Height Distribution of Surface Irregularities," *J. Am. Opt. Soc.* 53 (1963), p. 1389.

<sup>2</sup> D. Decker, "High Energy Laser Mirrors and Windows," Advanced Research Project Agency Order 2175, Semiannual Report No. 4, Sept. 1973 to March 1974.



TABLE 3. Relative Reflectance of Smooth and Rough Sputtered Titanium.

$\lambda$	$R_{\text{smooth}}$	$R_{\text{rough}}$
1.0	0.45115	0.11687
1.5	.49670	.18930
2.0	.53000	.26342
2.5	.56545	.31464
3.0	.63006	.40325
3.5	.69428	.47608
4.0	.74109	.52141
4.5	.77979	.58181
4.75	.79424	.61080
5.0	.80524	.63948
5.5	.82832	.68451
6.0	.84689	.72857
6.5	.85702	.75627
7.0	0.86824	0.78383

TABLE 4. Relative Reflectance of Smooth and Rough Sputtered Antimony.

$\lambda$	$R_{\text{smooth}}$	$R_{\text{rough}}$
1.0	0.59409	0.00000
1.5	.60812	.03414
2.0	.61856	.10993
2.5	.62318	.19481
3.0	.62906	.26579
3.5	.63405	.31912
4.0	.63949	.34696
4.5	.64681	.37690
4.7	.64900	.38531
4.75	.65007	.38684
4.8	.65113	.38817
5.0	.65492	.39520
5.5	.66674	.40629
6.0	.67797	.41814
6.5	.68815	.43001
7.0	0.69830	0.44249

They have an aspect ratio given by the ratio of the semiminor axis to the semimajor axis,  $a/b$ , shown in Figure 15. The analysis requires two physical conditions: (1) the polarizable oblate spheroid must have a large aspect ratio, and (2) the minor axis must lie in the direction of propagation of the incident light. These two factors are readily obtained in the rough sputtered films as seen by examination of the scanning electron micrographs.

The analysis proceeds by finding the amplitude of the incident and reflected intensities at the top of the oblate spheroid, see Figure 12 and Appendix A. The expression for the fractional decrease in reflectivity, Figure 16, is obtained after additional conditions are imposed and is given by

$$\frac{\Delta R}{R} = \frac{R_{\text{incident}} - R_{\text{reflected}}}{R_{\text{incident}}}$$

or

$$\frac{\Delta R}{R} = \frac{-32kap}{3} \frac{\epsilon_2 (L - 1)}{\{ [L(\epsilon_1 - 1) + 1]^2 + L^2 \epsilon_2^2 \}}$$

From the analysis in the appendix the condition which maximizes  $\Delta R/R$  is

$$L(\epsilon_1 - 1) + 1 = 0$$

Imposing the condition that  $|\epsilon_1| \gg 1$  leads to  $\epsilon_1 = -1/L$ , where  $L$  is the depolarization factor for the oblate spheroid and may be regarded as the slope,  $a/b$ . The appearance of a maximum is consistent with the spectral dependence of  $\epsilon_1$  and  $\epsilon_2$  for a free-electron metal, that is  $\epsilon_1$  is

negative for wavelengths greater than the bulk resonance wavelength and  $|\epsilon_1| \gg \epsilon_2$  in this region. These conditions generally prevail in the region where  $\lambda > 1$  micron. For silver the surface plasmon effect has been reported to occur at ultraviolet wavelengths (Figure 17).<sup>3</sup> The shift to longer wavelengths for titanium and antimony may be associated with greater effective masses for these materials since

$$\epsilon_1 = 1 - \frac{4\pi Ne^2}{m^*} \frac{1}{\left(\omega^2 + \frac{1}{\tau^2}\right)}$$

or

$$\epsilon_1 = 1 - \frac{\omega_p^2}{\left(\omega^2 + \frac{1}{\tau^2}\right)}$$

for a free-electron metal, a larger effective mass will shift the  $\epsilon_1$  versus  $\omega$  curve to lower values of  $\omega$ , hence to longer wavelengths. The condition of maximum reflectance for the resonant dipole model,

$$\epsilon_1 = \frac{-1}{L}$$

then occurs at longer wavelengths.

The magnitude of the  $\Delta R/R$  for the sputtered titanium and antimony films is expected to be greater than the values determined by Decker for aluminum films, Figure 18. An argument for greater magnitude can be made on the basis of a broad resonant dipole. Following Decker's analysis the depolarization factor  $L$  is associated with the slope of the oblate spheroid. Consideration of the effect of a distribution in slope,  $D(L)$ , leads to an expression for the average value of the change in reflectivity

$$\left\langle \frac{\Delta R}{R} \right\rangle = \int_0^\infty D(L) \frac{(\Delta R)}{R} dL.$$

From this one can say that when  $D(L)$  becomes large due to a large number of particles having slopes which contribute to the integration, then  $\langle \Delta R/R \rangle$  can be expected to be large. For rough sputtered films the number of particles having a distribution of slopes is considerable, as evidenced by the scanning electron micrographs for bismuth. For relatively smooth films the distribution in slopes is small and the number of particles contributing to the integration is small, so that  $\langle \Delta R/R \rangle$  is relatively unenhanced.

<sup>3</sup>T. Huen, G. Irani, F. Wooten. "Scanning Ultrahigh Vacuum Reflectometer," *Appl. Opt.* 10 (1971), p. 552.

The computation of the change in reflectivity from basic materials properties for rough films remains very intractable; however, characteristics associated with a broad resonant dipole model indicate the possibility of enhanced absorption in rough sputtered films.

## CONCLUSION

The decrease in reflectivity of bias sputtered titanium, bismuth, and antimony films shows a behavior that is explainable by scattering effects. In addition, an enhanced absorption in antimony and titanium in the intermediate infrared is possibly due to a broad resonant dipole mechanism.

Bias-sputtered films with rough surface texture appear to provide a means for studying absorption by surface plasmons since the effect may be enhanced in these films.

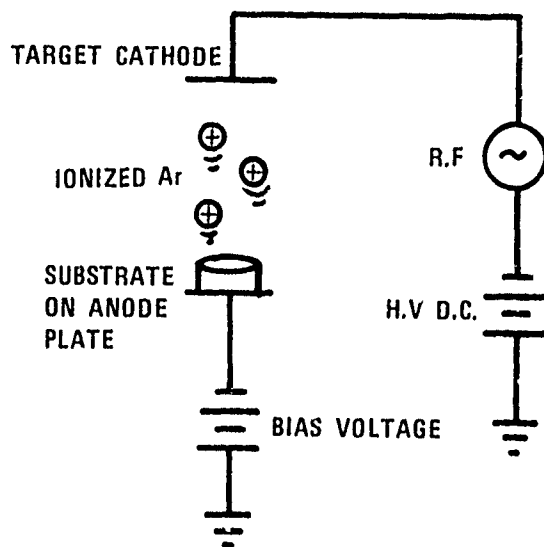


FIGURE 1. Schematic of Sputter Bias System.

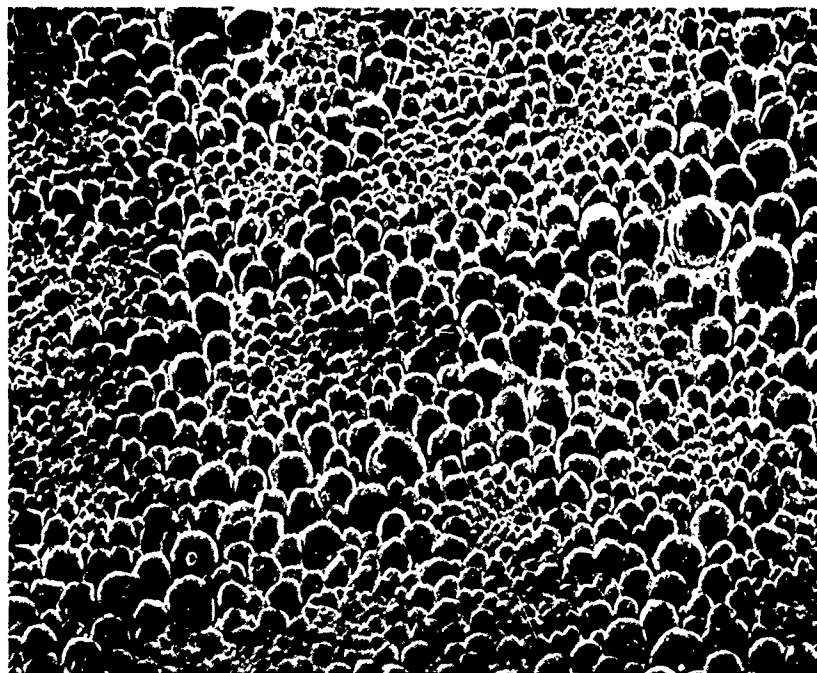


FIGURE 2. SEM Micrograph of Sputtered Bismuth Film, 400X. Bias voltage was zero and pressure  $3 \times 10^{-2}$  torr of argon. Average size of particle is 15 microns.



FIGURE 3. SEM Micrograph of Sputtered Bismuth, Same Film as Figure 2, but at 2100X.

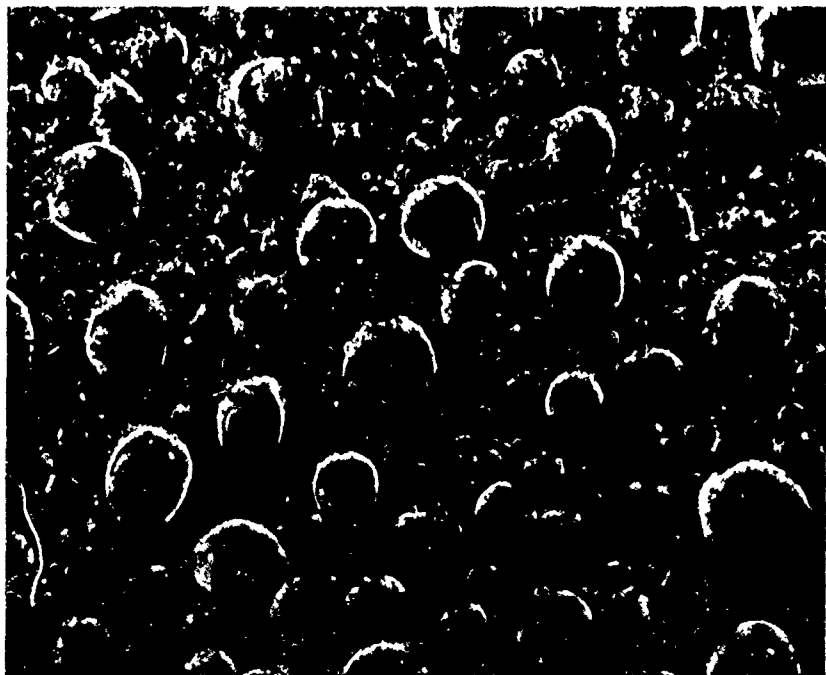


FIGURE 4. SEM Micrograph of Sputtered Bismuth Film 100X. Bias voltage was zero and pressure  $3 \times 10^{-2}$  torr of argon. Average diameter of larger particles is 127 microns.

NWC TP 5997

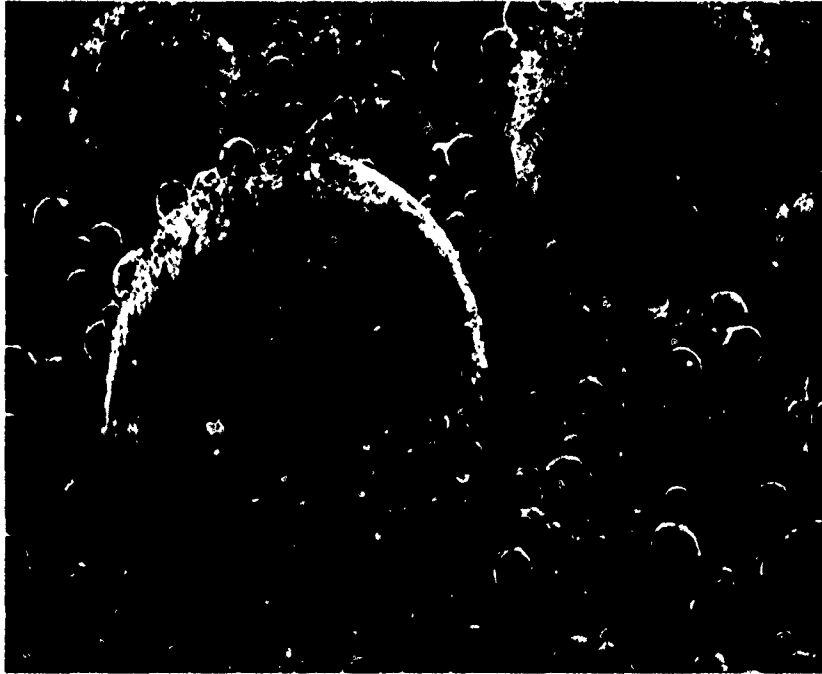


FIGURE 5. SEM Micrograph of Film Shown in Figure 4, but at 400X.



FIGURE 6. SEM Micrograph of Sputtered Bismuth on Sapphire Substrate, 400X. Average width of columnar protuberances is 12.5 microns.

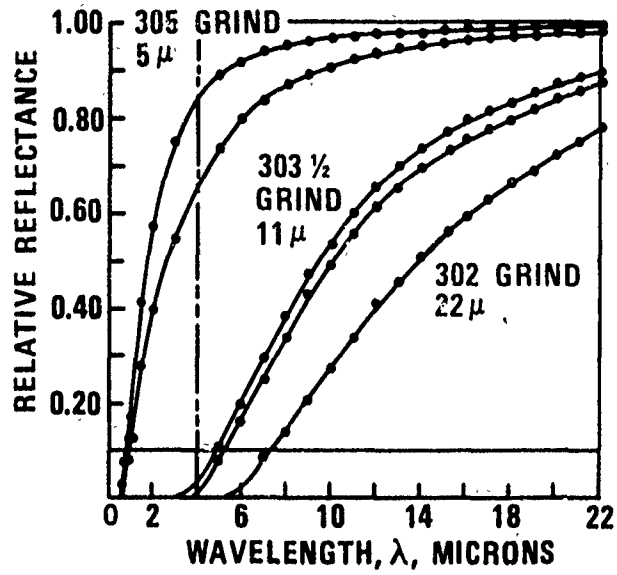


FIGURE 7. Effect of Intentionally Roughened Surface on Reflectivity of Aluminum.

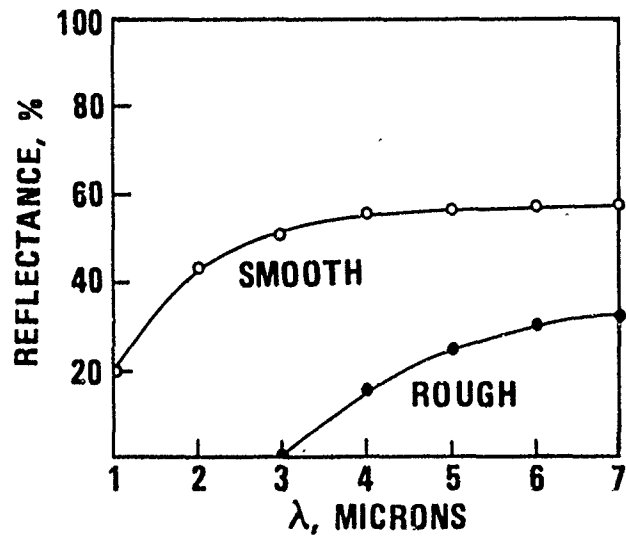


FIGURE 8. Reflectivity of Sputtered Bismuth.

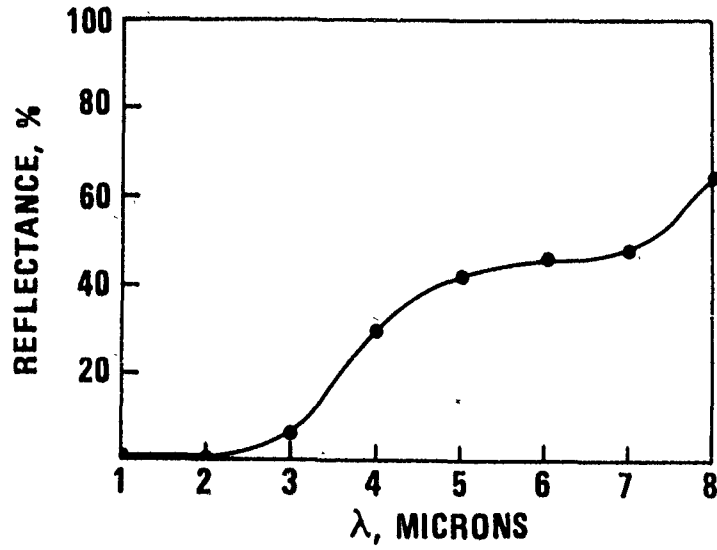


FIGURE 9. Reflectivity of Sputtered Copper.

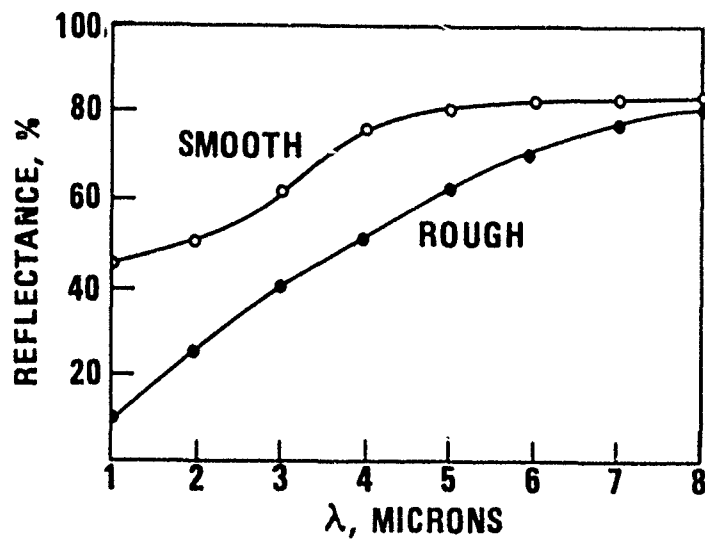


FIGURE 10. Reflectivity of Sputtered Titanium.



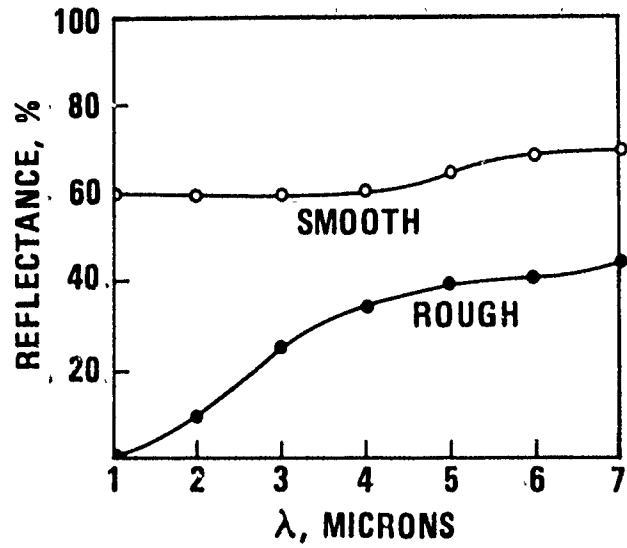


FIGURE 11. Reflectivity of Sputtered Antimony.

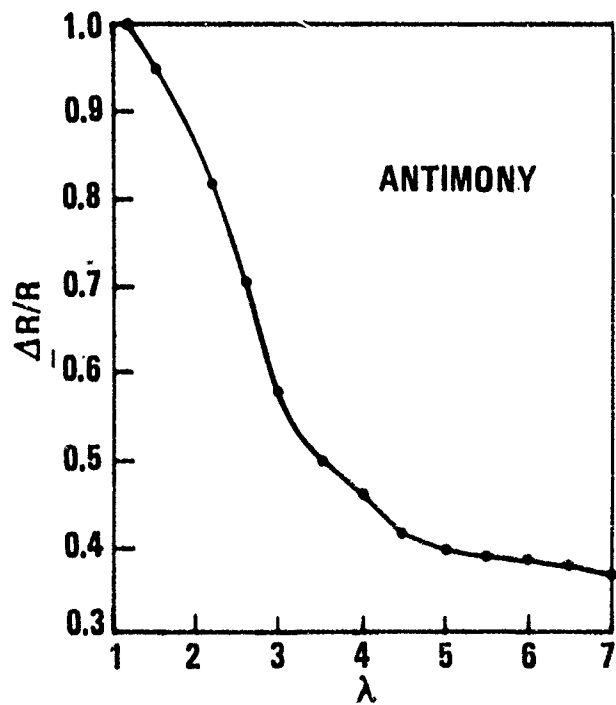


FIGURE 12. Relative Reflectance of Antimony.

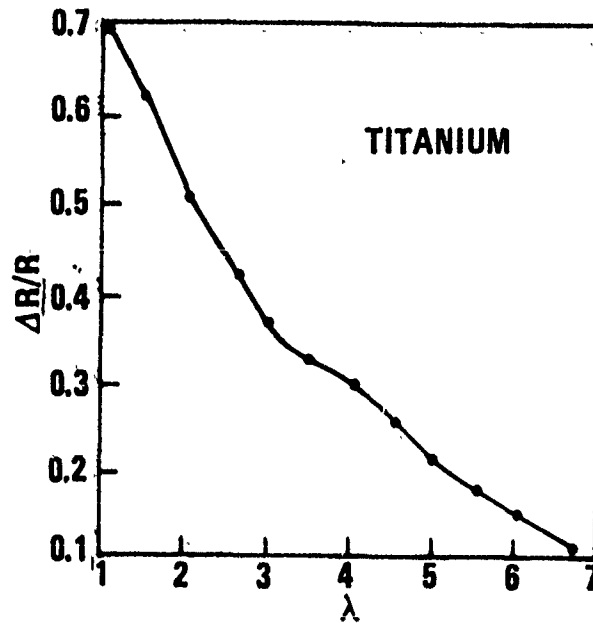


FIGURE 13. Relative Reflectance of Titanium.

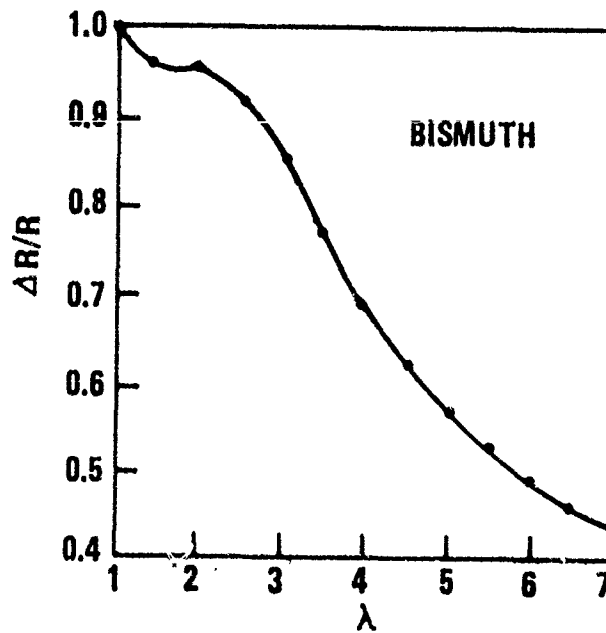


FIGURE 14. Relative Reflectance of Bismuth.

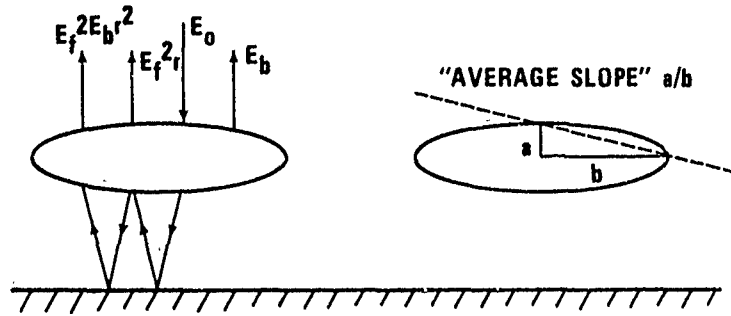


FIGURE 15. Oblate Spheroid of Resonant Dipole Absorption Model, After Decker.

$$E_f = E_0 \left[ 1 - \left( \frac{2\pi}{k^2} \right) n S_{(0)} \right]$$

$$E_b = -E_0 \left( \frac{2\pi}{k^2} \right) n S_{(180)}$$

$$\frac{\Delta R}{R} = \frac{|r_0|^2 - |r|^2}{|r_0|^2} \quad \text{(RELATIVE CHANGE IN REFLECTIVITY)}$$

$$\frac{\Delta R}{R} = -32 \frac{k a p}{3} \frac{\epsilon_2 (L + 1)}{\{ [L(\epsilon_1 - 1) + 1]^2 + L^2 \epsilon_2^2 \}}$$

WHERE

$$L \approx \frac{\pi}{4} \frac{a}{b}$$

$$p = \frac{\pi b^2 n}{2}$$

{ DEPOLARIZATION FACTOR FOR  
OBLATE SPHEROID I.E. SLOPE OF  
POLARIZABLE ELEMENT OF  
SURFACE }

$$\langle \frac{\Delta R}{R} \rangle = \int_0^\infty D_{(L)} \left( \frac{\Delta R}{R} \right) dL$$

FIGURE 16. Expressions Derived in Decker.

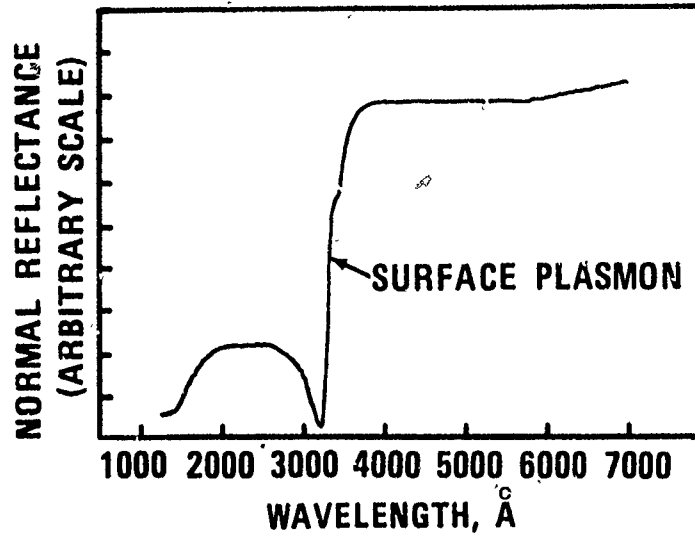


FIGURE 17. Surface Plasmon Effect in Silver.

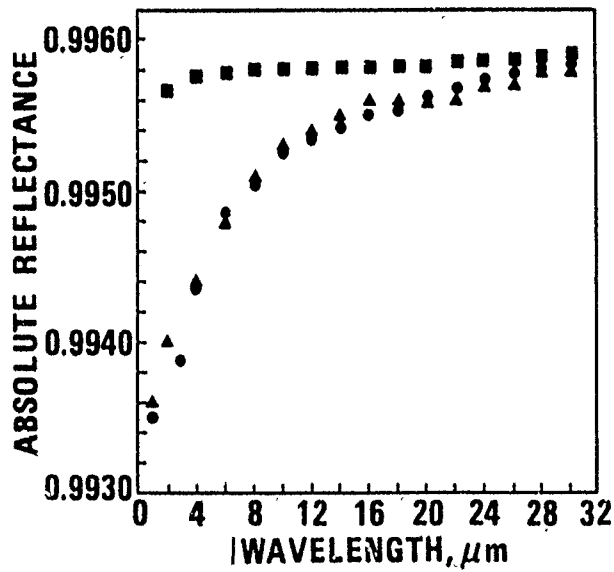


FIGURE 18. Reflectance for ■ Drude Model of Free-Electron Metal, ▲ Experimental Data Taken on Silver at NWC, and ● Drude Model With Addition of Resonant Dipole Absorption, From Decker.

Appendix A  
**OUTLINE OF THE BROAD RESONANT DIPOLE MODEL**

From Figure 15, which shows the incident and reflected electric field vectors for a single polarizable oblate spheroid, the electric fields due to a collection of  $n$  particles are given by

$$E_f = E_o \left[ 1 - \left( \frac{2\pi}{k_2} \right) n S_{(o)} \right]$$

for the forward direction and

$$E_b = -E_o \left( \frac{2\pi}{k_2} \right) n S_{(180)}$$

for the backward direction, where  $k$  is the wave vector,  $2\pi/\lambda$ , and  $S$  is the scattering amplitude factor.

Next the amplitude reflectance is computed and, imposing the condition that  $S_{(o)} = S_{(180)}$  when  $a$  is much less than the exciting wavelength, is reduced to

$$r = r_o \left\{ 1 - \frac{2\pi}{k_2} n S_{(o)} \frac{(1 + r_o)^2}{r_o} \right\}$$

The fractional decrease in reflectance due to resonant absorption is then expressed by

$$\frac{\Delta R}{R} = \frac{|r_o|^2 - |r|^2}{|r_o|^2}$$

Using the condition that the depolarization factor  $L_1$  for an oblate spheroid of large aspect ratio with the minor axis in the direction of the propagating electric field can be expressed as,

$$L = \frac{\pi a}{4 b}$$

and letting

$$p = \frac{\pi b^2 n}{2}$$

then after an appropriate amount of algebraic expansion and manipulation, keeping only terms to first order in  $ka$ , the fractional decrease in reflectance is expressed by,

$$\frac{\Delta R}{R} = \frac{-32kap}{3} \frac{\epsilon_2(L-1)}{\left\{ [L(\epsilon_1 - 1) + 1]^2 + L^2 \epsilon_2^2 \right\}}$$

Now  $\Delta R/R$  becomes maximum when

$$[L(\epsilon_1 - 1) + 1]^2 = 0$$

Let

$$|\epsilon_1| \gg 1 \quad \text{then} \quad G_1 - 1 \cong G_1 \quad \text{and} \quad L\epsilon_1 + 1 = 0$$

Now the condition for maximum  $\Delta R/R$  is  $L = -1/\epsilon_1$ . Note that  $\epsilon_1$  is a negative quantity for free-electron metals in the region of interest; hence  $L$  is a positive quantity, as it should be.

For a metal, the complex dielectric constant is given by  $\tilde{\epsilon} = \epsilon_1 + i\epsilon_2$

where

$$\epsilon_1 = 1 - \frac{\omega_p^2 \tau}{(1 + \omega^2 \tau^2)}$$

$$\epsilon_2 = \frac{\omega_p^2 \tau^2}{\omega(1 + \omega^2 \tau^2)}$$

$\tau \equiv$  mean free time between collisions of free electrons in the metal

$$\omega_p^2 = \frac{4\pi N e^2}{m^*} \quad \text{and}$$

$m^* \equiv$  effective mass of the electrons in the metal

From these relationships it can be shown that as  $m^*$  is increased the value of  $\omega$  at which  $L = -1/\epsilon_1$  decreases, and hence resonance occurs maximizing  $\Delta R/R$  at longer wavelengths.

The total absorption due to all elements acting in resonance is expressed by considering the average fractional change in reflectance,  $\langle \Delta R/R \rangle$ . When there is a distribution of slopes among these particles, this can be accounted for by considering a slope distribution function,  $D(L)$ .

Then

$$\left\langle \frac{\Delta R}{R} \right\rangle = \int_0^{\infty} D(L) \left( \frac{\Delta R}{R} \right) dL$$

INITIAL DISTRIBUTION

- 1 Chief of Navy Laboratories
- 9 Naval Air Systems Command
  - AIR-03B (1)
  - AIR-30212 (2)
  - AIR-350 (1)
  - AIR-954 (2)
  - ADPO-32A (1)
  - Dr. Mueller (1)
  - James Willis (1)
- 1 Chief of Naval Operations (OP-0982F4)
- 4 Chief of Naval Material
  - MAT-03 (1)
  - MAT-03PB (1)
  - MAT-032B (1)
  - NSP-001 (1)
- 4 Naval Sea Systems Command
  - SEA-034 (1)
  - SEA-09G32 (2)
  - PMS-405 (1)
- 6 Chief of Naval Research, Arlington
  - ONR-42C (1)
  - ONR-421 (1)
  - ONR-425 (1)
  - ONR-461 (1)
  - Dr. W. J. Condell, Jr. (1)
  - Dr. Robert Morris (1)
- 4 Naval Ocean Systems Center, San Diego
  - NELC
    - Dr. J. M. Hood, Jr. (1)
    - Dr. R. F. Potter (1)
    - Dr. Donald Stierwalt (1)
  - Code 1311 (1)
- 3 Naval Postgraduate School, Monterey
  - Dr. E. Crittenden (1)
  - Dr. W. F. Koehler (1)
  - Dr. J. Neighbours (1)
- 9 Naval Research Laboratory
  - Dr. Marvin Hass (1)
  - Dr. James Schulman (1)
  - Code 6503, Laser Technology Program
    - Dr. John MacCallum, Jr. (1)
    - Dr. W. R. Sooy (1)

NWC TP 5997

- W. R. Hunter (1)
- Code 6330 (1)
- Code 6506 (1)
- Code 6507, D. J. McLaughlin (1)
- Code 6530 (1)
- 8 Naval Surface Weapons Center, White Oak
  - Dr. J. Dixon (1)
  - Dr. R. Greene (1)
  - Dr. E. Leroy Harris (1)
  - Dr. W. Scanlon (1)
  - Dr. Leon H. Schindel (1)
  - K. Enkenhus (1)
  - J. Wise (1)
  - Technical Library (1)
- 1 Office of Naval Research Branch Office, Boston (Dr. Fred Quelle)
- 1 Office of Naval Research Branch Office, Pasadena (Dr. Robert Behringer)
- 2 Pacific Missile Test Center, Point Mugu
  - Code 5352, Gary Gibbs (1)
  - Technical Library (1)
- 1 Navy Laser Liaison Office, Kirtland Air Force Base (HELP-LO, Dr. John L. Walsh)
- 2 Office Chief of Research and Development
  - DARD-ARP-P, Dr. Watson (1)
  - DARD-MSA (1)
- 1 Army Combat Development Command, Air Defense Agency, Fort Bliss
- 1 Army Combat Development Command, Fort Leavenworth (Combat Systems Group, COL McFall)
- 1 Army Electronics Command, Fort Monmouth (AMSEL-XL-H, R. G. Buser)
- 2 Army Materiel Development and Readiness Command (AMCRD-TP)
  - Dr. B. Zarwyn (1)
  - Paul Chernoff (1)
- 3 Army Missile Research and Development Command, Redstone Arsenal
  - Research and Development Division
    - Dr. Tom Barr (1)
    - Dr. J. P. Hallows (1)
    - Walter Jennings (1)
- 1 Army Weapons Command, Rock Island Arsenal (SWERR-R, J. W. McGarvey)
- 2 Army Ballistic Missile Defense Program Office, Arlington
  - Chief, Intelligence and Security Office (1)
  - Albert J. Bast, Jr. (1)
- 3 Army Ballistics Research Laboratories, Aberdeen Proving Ground
  - Dr. E. C. Alcaez (1)
  - Dr. Robert Eichelberger (1)
  - Frank Allen (1)
- 3 Ballistic Missile Defense Advanced Technology Center, Huntsville
  - CRDABH-O (1)
  - RDMH-M, Dr. Ben Shratter (1)
  - Forney Hoke (1)



- 3 Redstone Arsenal
  - AMSMI-RRE, Dr. J. Bennett (1)
  - HEL Program Office, Dr. B. Jennings (1)
  - AMSMI-QPA, G. Hutcheson (1)
- 2 Air Force Systems Command, Andrews Air Force Base
  - DLTW, LTCOL Anthony J. Chiota (1)
  - XRLW, CAPT E. H. Cobb (1)
- 1 Air Force Aero-Propulsion Laboratory, Wright-Patterson Air Force Base
  - (CC, COL Walter Moe)
- 1 Air Force Avionics Laboratory, Wright-Patterson Air Force Base
  - (TEL, K. Hutchinson)
- 4 Air Force Cambridge Research Laboratories, Laurence G. Hanscom Field
  - Dr. John Garing (1)
  - Dr. A. Kahan (1)
- 1 Air Force Rocket Propulsion Laboratory, Edwards Air Force Base
  - (LKCG, B. R. Bornhorst)
- 1 Air Force Rocket Propulsion Laboratory, Edwards Air Force Base
  - (PYSP, CAPT S. Thompson)
- 2 Electronics Systems Division, Laurence G. Hanscom Field
  - XRJ, CAPT James C. Jalbert (1)
  - XRT, Alfred E. Anderson (1)
- 2 Foreign Technology Division, Wright-Patterson Air Force Base
  - PDTA (1)
  - PDTR (1)
- 1 Rome Air Development Center, Griffiss Air Force Base (Frank J. Rehm)
- 1 Space and Missile Systems Organization, Los Angeles (AFUPO, XRTD,  
LT Dorian DeMaio)
- 1 Assistant Secretary of Defense (Systems Analysis, Strategic Programs,  
Gerald R. Nichols)
- 2 Director of Defense Research and Engineering
  - Assistant Director I & C (1)
  - SW, Ben T. Plymale (1)
- 3 Defense Advanced Research Projects Agency, Arlington
  - Director, Laser Division (1)
  - MAJ Robert Paulsen (1)
  - Dr. Martin Stickley (1)
- 1 Arms Control and Disarmament Agency (Dr. Charles Henkin)
- 12 Defense Documentation Center
- 2 Ames Research Center
  - Dr. Kenneth Billman (1)
  - Robert L. McKenzie (1)
- 2 Goddard Space Flight Center
  - Dr. L. Dunkelman (1)
  - Dr. Fred Paul (1)
- 1 Lewis Research Center (Aerospace Research Engineer, Dr. John W. Dunning, Jr.)
- 2 AVCO Research Laboratory, Everett, MA

NWC TP 5997

- Dr. Jack Daugherty (1)  
Dr. George Sutton (1)
- 1 Aerospace Corporation, Los Angeles, CA (Dr. G. P. Millburn)  
1 Airesearch Manufacturing, Los Angeles, CA (A. Colin Stancliffe)  
1 Analytic Services, Inc., Falls Church, VA (Dr. John Davis)  
2 Applied Physics Laboratory, JHU, Laurel, MD  
    Dr. R. E. Gorozdos (1)  
    Dr. Albert Stone (1)
- 1 Atlantic Research Corporation, Alexandria, VA  
1 Autonetics/Rockwell International Corporation, Anaheim, CA  
    (Code HA18, T. T. Kumagai)
- 1 Battelle Memorial Institute, Columbus, OH (STOICAC, Fred Tietzel)  
2 Battelle Memorial Pacific Northwest Laboratories, Richland, WA  
    DSB 3000 Area, Dr. R. S. Gordon (1)  
    MET DEV Department 231F, R. W. Stewart (1)
- 1 Electro-Optical Systems, Inc., Pasadena, CA (Dr. Andrew Jensen)  
1 General Electric Company, Defense Electronics Division, Pittsfield,  
    MA (D. G. Harrington)
- 1 General Electric Company, Missile Space Vehicle Department,  
    Philadelphia, PA (Space Division, W. J. East)
- 1 General Research Corporation, Santa Barbara, CA (Dr. R. Holbrook)  
1 Hercules, Inc., Cumberland, MD (Dr. Ralph F. Preckel)  
1 Hercules, Inc., Research Center, Wilmington, DE (Industrial Systems  
    Department, Director, Systems Group, J. E. Greer)
- 1 Honeywell Corporate Research Center, Bloomington, MN (Research  
    Center, E. Bernal G.)
- 1 Hughes Aircraft Company, Canoga Park, CA (Aero-Space Group,  
    Systems Division, Dr. Jack A. Alcalay)
- 2 Hughes Aircraft Company, Culver City, CA  
    Dr. Eugene Peressini (1)  
    D-1281, James Rogers (1)
- 1 Hughes Aircraft Company, Fullerton, CA (Dr. William Yates)
- 3 Hughes Aircraft Company, Hughes Research Laboratories, Malibu, CA  
    Dr. Peter O. Clark (1)  
    Dr. D. Forster (1)  
    Morris Braunstein (1)
- 1 Institute for Defense Analyses, Arlington, VA (Dr. Alvin Schnitzler)  
1 Institute for Science and Technology, The University of Michigan,  
    Ann Arbor, MI (Dr. G. Zissis)
- 5 Lincoln Laboratory, MIT, Lexington, MA  
    Dr. R. S. Cooper (1)  
    Dr. G. P. Dinneen (1)  
    Dr. S. Edelberg (1)  
    Dr. J. Freedman (1)  
    Dr. R. Kingston (1)